

Second Harmonic Generation (SHG) Microscopy: The Forward-to-Backward (F/B) issue. (Dr. Rebecca Williams, Biomedical Engineering, Cornell University)

Because SHG is a coherent process, some type of phase matching must occur between different nonlinear scattering elements in the focal volume in order for signal to be strong enough to be detected. Neglecting linear scattering of SHG from outside the focal volume, the amount of forward to backward directed emission (F/B) is almost entirely determined by the axial extent of the nonlinearly scattering object with respect to the wavelength of light (λ). The linear analog of this principle is demonstrated in Mie vs. Rayleigh scattering (Figure 1).

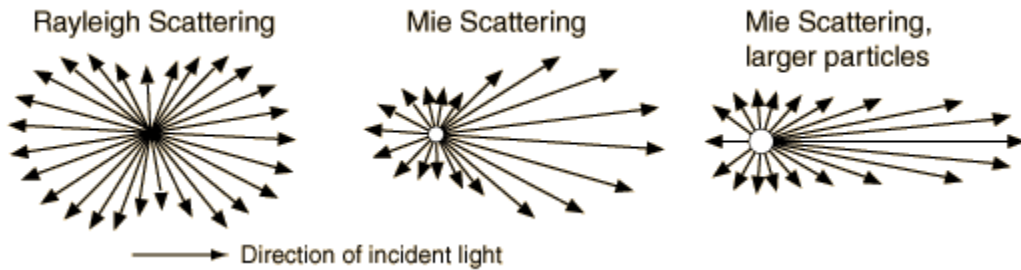
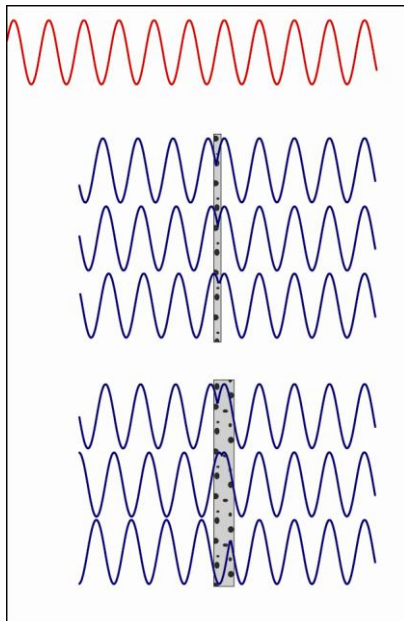


Figure 1: Particles that are small with respect to the wavelength scatter equivalently in forward and backward directions, whereas those that are larger tend to be mostly forward scattering (taken from <http://hyperphysics.phy-astr.gsu.edu/Hbase/atmos/imgatm/>.)



Mie identified this effect by integrating dipole radiators over varying sphere volumes with the use of Legendre polynomials (and without the use of computers, see Mie, 1908). However, the intuitive reason for the increased F/B of *thick* particles is depicted in the left diagram (Figure 2).

Figure 2. SHG from *thick* ($\sim\lambda$) vs. *thin* ($\ll\lambda$) specimens. The red wave represents the squared fundamental excitation. The blue waves represent SHG from thin (above) and thick (below) scattering specimens. Forward directed waves always phase match with forward directed waves. In contrast backward waves do not in general phase match with backward waves, because the oscillations that cause them are incited by and thus synchronized with the forward directed wave. Backward

directed waves only constructively interfere when there is no significant phase advance across the specimen (i.e. when the specimen is thin).

This concept has tremendous implications in SHG microscopy where scattering objects may or may not be small compared with the interrogation wavelength. Collagen fibril orientation generally has the largest effect on F/B (Figure 3a-c and Zipfel, Williams et al. 2003). For fibrils that were oriented uniformly laterally to the beam, an F/B analysis showed that collagen fibrils (in physiologic saline) scatter like tube-like rather than rod-like objects (Williams, Zipfel et al. 2005). Presumably because of varying shell thicknesses, mature collagen fibrils exhibit significantly higher F/B than immature segmental collagen (Figure 3d). Similar analyses exist for interpreting images from other biological SHG emitters, such as microtubules (Kwan, Dombeck et al. 2008) and skeletal myosin (Chu, Tai et al. 2009). The F/B issue must be accounted for not just in SHG microscopy, but in all the coherent nonlinear microscopies (for example see Volkmer, Cheng et al. 2001; Cheng, Volkmer et al. 2002).

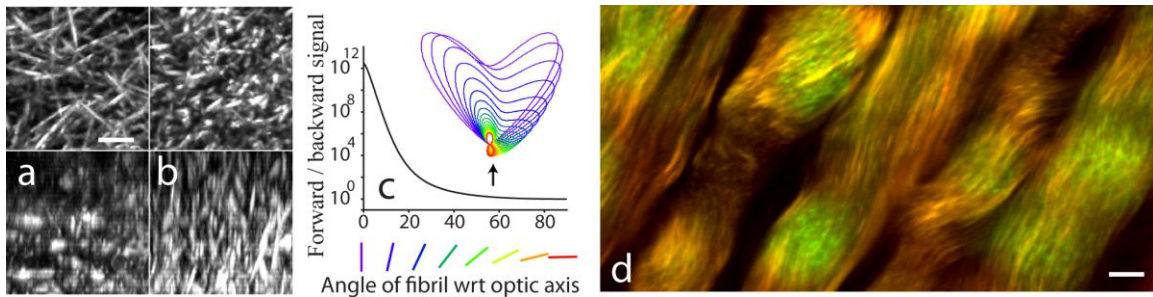


Figure 3. F/B issues in collagen microscopy. Fibril orientation is the primary issue in F/B determination. Simultaneously acquired backward (a) and forward (b) images yield complimentary images of a collagen gel. Shown are lateral (above) and axial (below) projections. Note that the laterally oriented fibrils appear primarily in the backward channel whereas the axial oriented fibrils appear primarily in the forward direction. As shown by this simulation of an infinitesimally thin fibril, the angle of the fibril with respect to the optic axis changes F/B by many orders of magnitude. d) In this image of growing tendon, immature segmental collagen appears primarily in the backward detection channel (green), whereas mature fibrils appear primarily in the forward channel. All scale bars are 5 μm .

As a footnote, we mention “traditional” phase matching associated with SHG crystals (i.e. as described in texts on laser optics). Discussions of crystal phase matching are associated with the fact that the fundamental and SHG waves lose phase as they travel through the nonlinear crystal due to a differing index of refraction of the two wavelengths. The coherence length of these two waves is given by: $L_C = \lambda_{SHG} / \pi \Delta n$ where Δn is the difference in refractive index between fundamental and SHG wavelengths. To our knowledge, the spectral dependence of tissue refractive index has never been measured; however, this value is typically $\Delta n = 0.015$ for water

($\lambda_{SHG} = 400 \text{ nm}$), leading to $L_C \approx 8 \mu\text{m}$. Therefore, this type of analysis (and the use of the usual set of equations) is only relevant for very low NA microscopy where the focal axial length is relatively long.

References cited

- Mie, G. (1908). "Articles on the optical characteristics of turbid tubes, especially colloidal metal solutions." Annalen Der Physik **25**(3): 377-445. (PMCIDISI:000201947800001)
- Volkmer, A., J. X. Cheng, et al. (2001). "Vibrational imaging with high sensitivity via epidetected coherent anti-Stokes Raman scattering microscopy." Physical Review Letters **87**02(2): 023901-1-4. (PMCIDISI:000169823100015)
- Cheng, J. X., A. Volkmer, et al. (2002). "Theoretical and experimental characterization of coherent anti-Stokes Raman scattering microscopy." Journal of the Optical Society of America B-Optical Physics **19**(6): 1363-1375. (PMCIDISI:000176205700018)
- Zipfel, W. R., R. M. Williams, et al. (2003). "Live tissue intrinsic emission microscopy using multiphoton excited intrinsic fluorescence and second harmonic generation." Proc Natl Acad Sci **100**(12): 7075-80.)
- Williams, R. M., W. R. Zipfel, et al. (2005). "Interpreting second-harmonic generation images of collagen I fibrils." Biophys J **88**(2): 1377-86. (PMCID15533922)
- Kwan, A. C., D. A. Dombeck, et al. (2008). "Polarized microtubule arrays in apical dendrites and axons." Proc Natl Acad Sci U S A **105**(32): 11370-5. (PMCID18682556)
- Chu, S. W., S. P. Tai, et al. (2009). "Selective imaging in second-harmonic-generation microscopy with anisotropic radiation." J Biomed Opt **14**(1): 010504. (PMCID19256686)